178 *Inorg. Chem.* **2011**, *50*, 178–192
DOI: 10.1021/ic1015884

Inorganic Chemistry
Article

Electronic Dimensions of FeMo-co, the Active Site of Nitrogenase, and Its Catalytic Intermediates

Ian Dance*

School of Chemistry, University of New South Wales, Sydney 2052, Australia

Received August 6, 2010

The iron−molybdenum cofactor (FeMo-co), which is the catalytic center for the enzymatic conversion of N_2 to NH_3, has the composition [NFe_7MoS_9(homocitrate)], and, with a cluster of eight transition metal atoms and nine sulfur atoms, has a complex delocalized electronic structure. The electronic dimensions of FeMo-co and of each of its derivatives appear as sets of electronic states lying close in energy. These electronic dimensions naturally partner the geometrical changes and the reactivity patterns during the catalytic cycle, and also connect with spectroscopic investigations of the mechanism. This paper describes straightforward computational procedures for the determination and management of the low-lying electronic states of FeMo-co and of its coordinated intermediates and transition states during density functional simulations of steps in the catalytic mechanism. General principles for the distribution of electron spin density over all atoms are presented, using several proposed intermediates as examples. A tough general irony arises in the distribution of spin density over FeMo-co and its derivatives: the less interesting atoms get the spin, and the most interesting atoms do not.

Introduction

The enzymatic reduction of N_2 to NH_3 occurs at the FeMo cofactor (FeMo-co) in nitrogenase.[1,2] The structure of FeMo-co is known,[3] Figure 1, but the chemical mechanism of the FeMo-co catalyzed transformation of N_2 to NH_3 under mild conditions is unknown.[2,4] Experimental investigations of the mechanism of this remarkable and complex reaction are proceeding with difficulty mainly because intermediates are difficult to trap.[2,5−7] Chemical synthesis of FeMo-co has not yet been achieved.[8]

The cluster at the core of FeMo-co has the composition XFe_7MoS_9, with ligation of one terminal Fe atom by cysteine, and ligation of the Mo atom at the other end by homocitrate and histidine. The identity of the central atom (X) is not confirmed experimentally, but all theoretical investigations[9−13] indicate that it is most likely N, and it will be labeled N^c hereafter. The central cluster core can be regarded as two cubanoid moieties sharing N^c, and further linked by three doubly bridging S atoms (S2B, S3A, S5A Figure 1). Alternatively FeMo-co is envisaged as a triangular prism of Fe atoms (Fe2−Fe7), centered with N^c, bridged on the three axial edges by μ-S atoms and on the six triangle edges by μ_3-S atoms. There is consensus that in the resting state of the enzyme the central cluster core of FeMo-co has the charge $[NFe_6MoS_9]^0$,[11−14] and the resting state of FeMo-co has overall spin $S = 3/2$. All of the contemporary experimental investigations of the mechanism of catalysis by FeMo-co indicate that the

*E-mail: i.dance@unsw.edu.au.

(1) Burris, R. H. *J. Biol. Chem.* **1991**, *266*(15), 9339–9342. Peters, J. W.; Fisher, K.; Dean, D. R. *Annu. Rev. Microbiol.* **1995**, *49*, 335–366. Burgess, B. K.; Lowe, D. *J., Chem. Rev.* **1996**, *96*, 2983–3011. Thorneley, R. N. F.; Lowe, D. J. *J. Biol. Inorg. Chem.* **1996**, *1*, 576–580. Howard, J. B.; Rees, D. C. *Chem. Rev.* **1996**, *96*, 2965–2982. Christiansen, J.; Dean, D. R.; Seefeldt, L. C. *Annu. Rev. Plant Physiol. Plant Mol. Biol.* **2001**, *52*, 269–295. Igarashi, R. Y.; Seefeldt, L. C. *Crit. Rev. Biochem. Mol. Biol.* **2003**, *38*(4), 351–384. Howard, J. B.; Rees, D. C. *Proc. Natl. Acad. Sci. U.S.A.* **2006**, *103*(46), 17119–17124.

(2) Seefeldt, L. C.; Hoffman, B. M.; Dean, D. R. *Annu. Rev. Biochem.* **2009**, *78*, 701–722.

(3) Einsle, O.; Tezcan, F. A.; Andrade, S. L. A.; Schmid, B.; Yoshida, M.; Howard, J. B.; Rees, D. C. *Science* **2002**, *297*, 1696–1700.

(4) Rees, D. C.; Tezcan, F. A.; Haynes, C. A.; Walton, M. Y.; Andrade, S.; Einsle, O.; Howard, J. A. *Phil. Trans. Roy. Soc. A* **2005**, *363*, 971–984.

(5) Dos Santos, P. C.; Igarashi, R.; Lee, H.-I.; Hoffman, B. M.; Seefeldt, L. C.; Dean, D. R. *Acc. Chem. Res.* **2005**, *38*(3), 208–214. Barney, B. M.; Lee, H.-I.; Dos Santos, P. C.; Hoffman, B. M.; Dean, D. R.; Seefeldt, L. C. *Dalton Trans.* **2006**, 2277–2284.

(6) Barney, B. M.; Lukoyanov, D.; Igarashi, R. Y.; Laryukhin, M.; Yang, T.-C.; Dean, D. R.; Hoffman, B. M.; Seefeldt, L. C. *Biochemistry* **2009**, *48* (38), 9094–9102.

(7) Hoffman, B. M.; Dean, D. R.; Seefeldt, L. C. *Acc. Chem. Res.* **2009**, *42* (5), 609–619.

(8) Groysman, S.; Holm, R. H. *Biochemistry* **2009**, *48*(11), 2310–2320.

(9) Dance, I. *Chem. Commun.* **2003**, 324–325.

(10) Hinnemann, B.; Norskov, J. K. *J. Am. Chem. Soc.* **2003**, *125*, 1466–1467.

(11) Vrajmasu, V.; Munck, E.; Bominaar, E. L. *Inorg. Chem.* **2003**, *42*(19), 5974–5988.

(12) Lovell, T.; Liu, T.; Case, D. A.; Noodleman, L. *J. Am. Chem. Soc.* **2003**, *125*, 8377–8383.

(13) Dance, I. *Inorg. Chem.* **2006**, *45*(13), 5084–5091.

(14) Schimpl, J.; Petrilli, H. M.; Blochl, P. E. *J. Am. Chem. Soc.* **2003**, *125*, 15772–15778.

Published on Web 12/08/2010

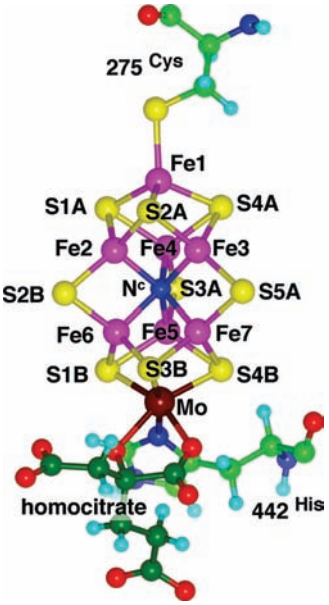

Figure 1. Structure of FeMo-co, linked to the protein through cysteine coordinated at Fe1 and histidine coordinated at Mo. Homocitrate (C atoms dark green) chelates Mo. Atom and residue labeling is that of Protein Database code 1M1N.[3].

central Fe atoms Fe2 and Fe6 are the most probable sites for binding of N_2 and other substrates.[2,5,15−18]

There have been many theoretical investigations of FeMo-co and its reactivity.[9,12−14,19−30] Theoretical investigations of the full mechanism of chemical catalysis effected by FeMo-co have resulted in three categories of mechanism, involving (a) major disruption of FeMo-co during the cycle,[31] or (b) partial disruption of FeMo-co,[14,23−25] or, most recently, (c) minimal change in the structure of FeMo-co during the catalytic cycle.[32,33] Some theoretically derived mechanisms invoke exogenous protonation of bound substrate and intermediates, while an alternative involving intramolecular hydrogenation, probably with hydrogen tunnelling,[34] has been argued strongly.[20,21,33]

This paper is concerned with the electronic structure of FeMo-co and of some of its ligated forms, and with the management of electronic states during computer simulation of the reactions of FeMo-co. With eight transition metal atoms and nine S atoms, the electronic structure of FeMo-co is expected to be complicated. Many d electrons are involved: although allocation of individual atomic oxidation states is questionable, if the resting state is described as $(N^{3-})(Fe^{3+})_3(Fe^{2+})_4(S^{2-})_9(Mo^{4+})$ the total number of metal d-electrons is 41. As a poly metal sulfide cluster, FeMo-co is considered to possess delocalized polar covalent bonding and to be electronically soft: Mulliken partial charges are about +0.6 on Fe, about +1.0 on Mo, and about −0.6 on S (partial charges on Fe calculated by the Hirshfeld method are much smaller, $< +0.1$).

Calculations of resting FeMo-co reveal that there are about 30 spin orbitals (in the unrestricted spin description) from 1 eV below the highest occupied molecular orbital (HOMO) to 1 eV above the HOMO, and the HOMO−LUMO gap is generally 0.2 to 0.6 eV. This gives rise to numerous electronic states for FeMo-co and derivatives, often quite close in energy. The electronic states are distinguished and described by their distributions of spin densities (sign and magnitude) on the individual Fe and Mo atoms, and by the total molecular spin (S).

The early density functional theory (DFT) calculations of FeMo-co and substrate-bound derivatives by Rod and Norskov[35] started with nonzero spin densities on each metal atom. Noodleman et al. describe the electronic states of FeMo-co in terms of "broken symmetry states" (terminology originally applied to systems with otherwise equivalent transition metal atoms,[36] but subsequently applied widely to systems with no molecular symmetry[37]).[12,26,28,30] The theoretical formulation for the broken symmetry description of electronic states in metal sulfide clusters is conceived in terms of metal ions with formal oxidation states and spin states, and with ferro- or antiferro-magnetic coupling of these atom-localized spins. The theory is relatively complex, with multiple parameters.[38] The procedure for calculation of the broken symmetry electronic states starts with an unrestricted calculation of the maximum

(15) Benton, P. M. C.; Laryukhin, M.; Mayer, S. M.; Hoffman, B. M.; Dean, D. R.; Seefeldt, L. C. *Biochemistry* **2003**, *42*, 9102–9109. Barney, B. M.; Igarashi, R. Y.; Dos Santos, P. C.; Dean, D. R.; Seefeldt, L. C. *J. Biol. Chem.* **2004**, *279*(51), 53621–53624. Igarashi, R.; Dos Santos, P. C.; Niehaus, W. G.; Dance, I. G.; Dean, D. R.; Seefeldt, L. C. *J. Biol. Chem.* **2004**, *279*(33), 34770–34775. Seefeldt, L. C.; Dance, I. G.; Dean, D. R. *Biochemistry* **2004**, *43*(6), 1401–1409. Dos Santos, P. C.; Mayer, S. M.; Barney, B. M.; Seefeldt, L. C.; Dean, D. R. *J. Inorg. Biochem.* **2007**, *101* (11−12), 1642–1648. Sarma, R.; Barney, B. M.; Keable, S.; Dean, D. R.; Seefeldt, L. C.; Peters, J. W. *J. Inorg. Biochem.* **2010**, *104*, 385–389.

(16) Barney, B. M.; Yang, T.-C.; Igarashi, R.; Dos Santos, P. C.; Laryukhin, M.; Lee, H.-I.; Hoffman, B. M.; Dean, D. R.; Seefeldt, L. C. *J. Am. Chem. Soc.* **2005**, *127*, 14960–14961.

(17) Igarashi, R. Y.; Laryukhin, M.; Dos Santos, P. C.; Lee, H.-I.; Dean, D. R.; Seefeldt, L. C.; Hoffman, B. M. *J. Am. Chem. Soc.* **2005**, *127*(17), 6231–6241.

(18) Barney, B. M.; McClead, J.; Lukoyanov, D.; Laryukhin, M.; Yang, T. C.; Dean, D. R.; Hoffman, B. M.; Seefeldt, L. C. *Biochemistry* **2007**, *46* (23), 6784–6794.

(19) Szilagyi, R. K.; Musaev, D. G.; Morokuma, K. *THEOCHEM* **2000**, *506*, 131–146. Szilagyi, R. K.; Musaev, D. G.; Morokuma, K. *Inorg. Chem.* **2001**, *40*, 766–775. Dance, I. *J. Am. Chem. Soc.* **2004**, *126*(36), 11852–11863. Dance, I. *J. Am. Chem. Soc.* **2007**, *129*(5), 1076–1088. Noodleman, L.; Han, W.-G. *J. Biol. Inorg. Chem.* **2006**, *11*(6), 674–694. Peters, J. W.; Szilagyi, R. K. *Curr. Opin. Chem. Biol.* **2006**, *10*(2), 101–108. Cao, Z.; Zhou, Z.; Wan, H.; Zhang, Q. *Int. J. Quantum Chem.* **2005**, *103*, 344–353. Cao, Z. X.; Jin, X.; Zhang, Q. N. *J. Theor. Comput. Chem.* **2005**, *4*, 593–602. Xie, H. J.; Wu, R. B.; Zhou, Z. H.; Cao, Z. X. *J. Phys. Chem. B* **2008**, *112*(36), 11435–11439.

(20) Dance, I. *J. Am. Chem. Soc.* **2005**, *127*, 10925–10942.

(21) Dance, I. *Biochemistry* **2006**, *45*(20), 6328–6340.

(22) Dance, I. *Chem. Asian J.* **2007**, *2*, 936–946.

(23) Kastner, J.; Blochl, P. E. *Inorg. Chem.* **2005**, *44*, 4568–4575. Kastner, J.; Blochl, P. E. *ChemPhysChem* **2005**, *6*, 1–4. McKee, M. L. *J. Comput. Chem.* **2007**, *28*(8), 1342–1356.

(24) Kastner, J.; Hemmen, S.; Blochl, P. E. *J. Chem. Phys.* **2005**, *123*(7), 074306.

(25) Kastner, J.; Blochl, P. E. *J. Am. Chem. Soc.* **2007**, *129*(10), 2998–3006.

(26) Lovell, T.; Li, J.; Liu, T.; Case, D. A.; Noodleman, L. *J. Am. Chem. Soc.* **2001**, *123*, 12392–12410.

(27) Lovell, T.; Li, J.; Case, D. A.; Noodleman, L. *J. Biol. Inorg. Chem.* **2002**, *7*, 735–749.

(28) Lovell, T.; Torres, R. A.; Han, W.-G.; Liu, T.; Case, D. A.; Noodleman, L. *Inorg. Chem.* **2002**, *41*, 5744–5753.

(29) Lukoyanov, D.; Pelmenschikov, V.; Maeser, N.; Laryukhin, M.; Yang, T. C.; Noodleman, L.; Dean, D. R.; Case, D. A.; Seefeldt, L. C.; Hoffman, B. M. *Inorg. Chem.* **2007**, *46*(26), 11437–11449.

(30) Pelmenschikov, V.; Case, D. A.; Noodleman, L. *Inorg. Chem.* **2008**, *47*(14), 6162–6172.

(31) Huniar, U.; Ahlrichs, R.; Coucouvanis, D. *J. Am. Chem. Soc.* **2004**, *126*, 2588–2601.

(32) Dance, I. *Mol. Simul.* **2008**, *34*(10), 923–929.

(33) Dance, I. *Dalton Trans.* **2008**, 5977–5991.

(34) Dance, I. *Dalton Trans.* **2008**, 5992–5998.

(35) Rod, T. H.; Norskov, J. K. *J. Am. Chem. Soc.* **2000**, *122*, 12751–12763.

(36) Noodleman, L.; Case, D. A.; Aizman, A. *J. Am. Chem. Soc.* **1988**, *110*, 1001–1005.

(37) Lovell, T.; Himo, F.; Han, W.-G.; Noodleman, L. *Coord. Chem. Rev.* **2003**, *238*, 211–232.

(38) Noodleman, L.; Peng, C. Y.; Case, D. A.; Mouesca, J. M. *Coord. Chem. Rev.* **1995**, *144*, 199–244.

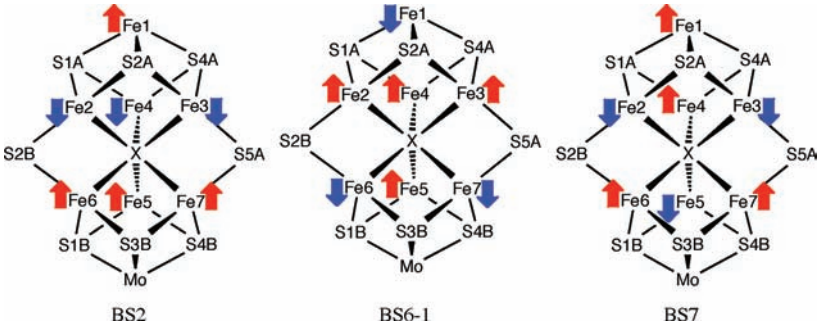

Figure 2. Alignments of the Fe spins for the three more stable electronic states of FeMo-co, as calculated by Lovell et al.[12,26,29] and by Blochl et al.[14,25] X was variable (C, N, or O) or absent in these calculations.

spin state, in which all d-electron spins are parallel. Then blocks of α and β electron densities in the maximum spin state are interchanged, to construct the various combinations that possess the lower desired total spin state for the cluster. These constructions are then optimized to self-consistent-field (scf) convergence. The first calculations for FeMo-co were made prior to knowledge of the existence of the central atom. Assuming that FeMo-co is composed of one low-spin Mo^{4+} (d^2), one Fe^{3+} (high-spin d^5, $S = 5/2$), and six Fe^{2+} (high-spin d^2, $S = 2$), and assuming C_3 symmetry for the cluster, Noodleman et al. described ten broken symmetry states (labeled BS1 to BS10) for resting FeMo-co with molecular spin $S = 3/2$.[26] The relative energies and geometries were calculated, and, on the basis of additional calculations incorporating the protein surrounds, one state (BS6) was concluded to be the ground state. These authors also noted that with removal of the assumption of 3-fold symmetry, 26 different electronic states would exist in the framework of their model. Subsequently, when the light atom at the center of FeMo-co was revealed, Lovell et al. recalculated the BS6 spin alignment[12] and BS7 spin alignment[29] states of FeMo-co with C, N or O as the light atom. These calculations for centered FeMo-co used a different collection of metal ions for FeMo-co, namely, $Mo^{4+}4Fe^{2+}3Fe^{3+}$, with a different sum of all spins, $S = 31/2$ rather than 29/2.

Blochl and Kastner et al. have also discussed the alignments of the spin densities of the seven Fe atoms of FeMo-co, first reporting one of the C_3 rotational isomers of BS7 as the resting state,[14] and subsequently adopting the alignment of BS7 (see Figure 2) in their computed mechanism for the conversion of N_2 to NH_3.[25] The alignments of the localized Fe spins in the three more stable electronic states of resting FeMo-co, BS2, BS6−1, and BS7, common to the calculations of Noodleman et al.[12,26,29] and Blochl et al.,[14,25] are shown in Figure 2. Further detail has been provided for the BS states for FeMo-co reduced by two electrons, and coordinated by allyl alcohol.[30]

Noodleman et al. use the Amsterdam density functional (ADF) platform for their calculations, with Slater-type basis sets. Norskov et al.,[10,35,39,40] and Blochl et al., use a plane-wave method, with well-separated periodic occurrences of each structure.[14,24,25] Blochl et al. have emphasized the use of noncollinear spins in determining the electronic ground state without the need for trial calculations of alternative spin orientations.[14]

My calculations of FeMo-co and its reactions involve numerical basis sets,[41] as implemented in the program DMol.[42] Control of electronic states in DMol can be effected through the specification of signed atomic spin densities prior to the scf calculation. The overall molecular spin state is controlled by specification of the numbers of α and β electrons in the spin-unrestricted calculation. In my published work on FeMo-co[32−34] the electronic states have been controlled while simulating reaction trajectories and reaction pathways, but full details of the electronic states and of the DMol methodology have not yet been published.

This paper has two main goals. The first is to describe in more detail than previously the methodologies used to control electronic and spin states during simulations of the reactions of FeMo-co. The second goal is to describe relationships between (a) electronic state, (b) distribution of spin density, (c) geometry, and (d) energy, and to extract from these relationships any principles that can guide future investigations. This is done for FeMo-co, and for three quite different but representative ligated forms of FeMo-co proposed as intermediates in reactions catalyzed by FeMo-co, to assess the range of relationships between (a), (b), (c), and (d) above. More specifically, FeMo-co coordinated at one or more of the central six Fe atoms changes N^c−Fe distances (this is communication between Fe atoms via N^c, called coordinative allosterism[22]), and relationships between these changes and electronic state are explored here. In addition, ligation of the Fe atoms of FeMo-co is associated with changes in their spin density, and an understanding of these changes is vital in interpretation of spectroscopic properties affected by spin density at Fe. Further, while most spin density resides on the metal atoms of ligated FeMo-co, some spin is delocalized onto ligand atoms, and an understanding of the magnitudes of this delocalization is essential in interpretation of spectroscopic properties which depend on electron spin density at ligand atoms. This paper is not a comprehensive account, and does not discuss mechanism, but seeks to provide general insight into these fundamental properties of reacting FeMo-co.

Methodology

The calculations use DMol[3,41−43] version 5.0, run in standalone mode outside of the Materials Studio interface.[44] The calculations are spin unrestricted, without scalar relativity corrections. The functional is BLYP.[45] The basis set is "dnp"

(39) Hinnemann, B.; Norskov, J. K. *J. Am. Chem. Soc.* **2004**, *126*, 3920–3927.
(40) Hinnemann, B.; Norskov, J. K. *Phys. Chem. Chem. Phys.* **2004**, *6*, 843–853.
(41) Delley, B. *J. Chem. Phys.* **1990**, *92*(1), 508–517.
(42) Delley, B. *J. Chem. Phys.* **2000**, *113*(18), 7756–7764.
(43) Delley, B. DMol, a standard tool for density functional calculations: review and advances. In *Modern density functional theory: a tool for chemistry*; Seminario, J. M., Politzer, P., Eds.; Elsevier: Amsterdam, 1995; Vol. *2*, pp 221−254.
(44) *DMol3*; accelrys.com/products/datasheets/dmol3.pdf, 2010; accelrys.com/products/materials-studio/publication-references/dmol3-references/index.html, 2010.
(45) Becke, A. D. *Phys. Rev. A* **1988**, *38*, 3098–3100. Lee, C.; Yang, W.; Parr, R. G. *Phys. Rev. B* **1988**, *37*, 785–789.

(double numerical basis set with d-polarization functions, and p-polarization for H),[41] which extends to 2p for H, 3d for C, N, O, S, 4p for Fe, and 5p for Mo. All orbitals are calculated: no frozen-core or pseudopotential approximations are used. The numerical integration grid quality is "fine": the radial cutoff parameter[42] Atom_Rcut was 9 au (4.76 Å): larger values make negligible difference. Validations of this methodology have been published previously.[13,20,46]

The calculated model of FeMo-co is **FeMoco-1**, with cysteine approximated as SCH_3, histidine replaced by imidazole, and homocitrate simplified to glycolate, maintaining the essential coordination of Fe1 and Mo. The net charge 3− for **FeMoco-1** corresponds to the resting state of FeMo-co. A total of 594 valence orbitals are included in the calculation of **FeMoco-1**.

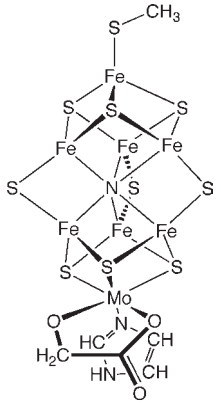

FeMoco-1

The overall molecular spin state (S) is controlled by specification of the (fixed) numbers of α and β electrons (input "Occupation" = fixed). The electronic states are controlled by input specification of trial spin densities on selected atoms (input parameter 'Start-Spin_Populations'). These are called "pre-scf" spin densities, defining a starting point for the scf calculation. In general an scf convergence criterion of 10^{-6} was used, but for some pre-scf trials this had to be relaxed in early stages to permit the electronic state to stabilize. All calculations were completed with scf convergence to 10^{-6}, and optimization of energy and geometry. On completion, Mulliken and Hirshfeld spin densities were calculated: the Hirshfeld values are about 10% smaller magnitude than the Mulliken results, which are reported here. Each calculation uses three input files: (a) the Cartesian coordinates (.car), (b) the orbital occupancy (α/β) file (.occup), (c) the input parameters (.input).

This methodology allows straightforward and easy exploration of electronic states (ES) and overall spin states (S). The electronic states are defined by their sets of signed atomic spin densities: these are named "spin-sets" in the following descriptions.

Regarding uncertainties in the reported calculations, the underlying DFT method, and functional used, cause the calculations to be slightly underbinding, with calculated distances up to 0.05 Å long: where relevant energy data are available for validation, the uncertainties in calculated energies are about 1−2 kcal mol^{-1}.[20] Relative errors in geometry and energy, relevant for the discussion below and for simulations of the reactions of FeMo-co, are smaller. Absolute errors in the calculated spin densities are probably about 10%.

(46) Dance, I. G. Computational Methods for Metal Sulfide Clusters. In *Transition Metal Sulfur Chemistry: Biological and Industrial Significance*; Stiefel, E. I., Matsumoto, K., Eds.; American Chemical Society: Washington, DC, 1996; Vol. *653*, pp 135−152; Dance, I. *J. Chem. Soc., Chem. Commun.* **1998**, 523–530.

Results

My exploration of electronic states is formulated in terms of different combinations of the signs of the spin densities on the metal atoms. With eight transition metals each able to adopt appreciable spin density of either sign, the total number of spin-sign combinations is large. With long experience in calculation of spin densities for FeMo-co and derivatives, it was evident that some spin-sign combinations would be very unfavorable, and/or incompatible with the overall molecular spin state S. Therefore exhaustive exploration was curtailed, according to some prior knowledge. Reasonable pre-scf magnitudes for the metal atom spin densities were also known, but as will be seen these magnitudes are not critical input.

Results are presented first for FeMo-co, then for two different significant intermediates in the proposed mechanism[33] for hydrogenation of N_2 to NH_3, and finally for an intermediate where relatively low-energy variation of SH conformations is possible, to develop another aspect of the connection between geometry and electronic state. For each compound the electronic states are labeled ESn, strictly in order (n) of decreasing stability; this means that for different species there is no correlation of these ESn labels and their spin-sets. The patterns of spins implicit in the BSn labels used elsewhere are not imposed here. Coordinates for all calculated structures are available from the author.

FeMo-co. For the observed $S = 3/2$ resting state, 35 distinct electronic states (ESn, $n = 1-35$) were calculated. The relative energies are shown in Figure 3. Twenty-two of these electronic states are within 11 kcal mol^{-1} of the lowest energy state. For the first 17 of the energy-ranked $S = 3/2$ electronic states, the same-spin-sets (i.e., the spin-sign combinations for $n = 1-17$) were optimized also for $S = 1/2$ and $S = 5/2$ total molecular spin, and the energies of these are also plotted in Figure 3. For each of these spin-sets the $S = 1/2$ and $S = 5/2$ states are less stable than the $S = 3/2$ state. The lowest energy electronic state with $S = 1/2$ has energy +5 kcal mol^{-1}, and the lowest energy electronic state with $S = 5/2$ has energy +7 kcal mol^{-1}. The calculated stabilization of $S = 3/2$ spin states over $S = 1/2$, $S = 5/2$ alternatives, evident in Figure 3, is consistent with the experimental observation of $S = 3/2$ for resting FeMo-co, and the following descriptions and discussion refer only to calculated $S = 3/2$ molecular spin states.

The magnitudes of the spin densities on Fe are generally 2.6 to 3.2e. The spin density of Fe1 is usually slightly larger than those of the other Fe atoms, and is charted in Figure 4. At Mo the spin densities are generally 0.3 to 0.4e, although in ES9 it is 1.0e (see Figure 4). Spin density is also dispersed onto non-metal atoms of FeMo-co, and the sum of the magnitudes of the non-metal spin densities is greater than 0.5 and near 1.0 in many of the more stable electronic states (see Figure 4). Further details of atomic spin densities are described below, after analysis of the spin-sign combinations in the more stable electronic states.

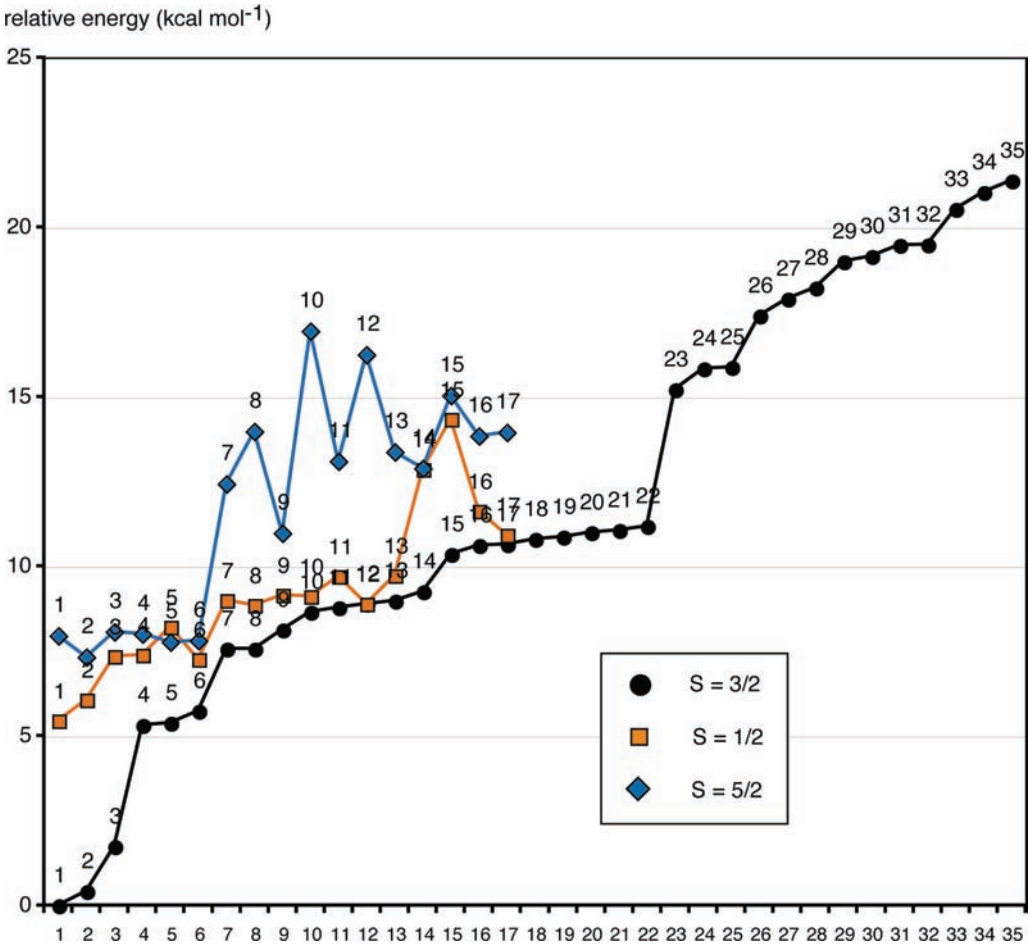

Figure 3. Relative energies (kcal mol^{-1}) of optimized electronic states of FeMo-co. Black symbols represent states with $S = 3/2$, the observed resting spin state, while orange ($S = 1/2$) and blue ($S = 5/2$) symbols are the energies of the optimized alternative molecular spin states with the same numbered atomic spin-sign sets as those for $S = 3/2$. The connecting lines provide visual aid and have no physical meaning.

The spin densities on Fe and Mo for ESn, $n = 1-9$ ($S = 3/2$) are presented in Table 1 (all results are available in the Supporting Information). Analysis of the metal spin-sets that yield these more stable electronic states of FeMo-co is made in terms of three component moieties: the Fe1−Fe2−Fe3−Fe4 cubanoid moiety (abbreviated to "Fe1-cubane"), the Fe5−Fe6−Fe7−Mo cubanoid moiety (abbreviated to "Mo-cubane"), and the N-centered Fe2−Fe3−Fe4−Fe5−Fe6−Fe7 prismane moiety. The three low energy states, ES1, ES2, and ES3, have 2 + 2− combinations of spin signs in each of the cubanoid moieties and antiparallel combinations on the three axial edges of the prismane. Electronic states ES4, ES5, and ES6 have 3 + 1− signs in Fe1 cubane, 2 + 2− signs in Mo cubane, and two rather than three antiparallel combinations on prismane edges. Electronic states ES7, ES8, ES10, ES11, ES12, ES13 have 2 + 2− combinations in each of the cubanes, and two antiparallel combinations on prismane edges. From this it is concluded that the most stabilizing properties of metal spin-sign combinations are (a) antiparallel +− along the prismane axial edges (Fe2−Fe6, Fe3−Fe7, Fe4−Fe5), and (b) 2 + 2− in the cubanes, and that (a) is more stabilizing than (b). The electronic states ES9, ES14, and ES15 each have three antiparallel prismane edges, but with conflicts in the cubane moieties which cause irregular spin magnitudes. In ES9 there is 3−1+ in the Fe1-cubane, 3 + 1− in the Mo-cubane, but with the consequence that the spin of Mo is anomalously large. In ES14 and ES15 the Fe1-cubane is 3 + 1− and the Mo-cubane is 2 + 2−, but only with diminished Fe1 spins (see Figure 4). From this behavior of ES9, ES14, and ES15 and all preceding electronic states it is concluded that spin magnitudes of about 3.2e for Fe1 and about 0.4 for Mo are most stabilizing. The lesser stabilities for the spin-sign combinations of the electronic states beyond ES15 can be interpreted in terms of absences of the above-mentioned stabilizing principles.

The Fe spin-sign combination of ES1 is the same as that of the BS7 state, and the magnitudes of the spin densities are similar although generally smaller as calculated by the BS/ADF methodology compared with the ES/DMol methodology. Specifically, ES1 values compared with BS7 values[29] in parentheses are: Fe1 +3.11 (+2.91); Fe2 −2.89 (−2.60); Fe3 +2.97 (+2.84); Fe4 −2.87 (−2.61); Fe5 +2.73 (+2.41); Fe6 +2.70 (+2.40); Fe7 −2.75 (−2.55). Hinnemann et al. reported spin densities of 1.5−3 on Fe.[39]

How is spin density distributed over non-metal atoms in the most stable electronic states of $S = 3/2$ FeMo-co? A key result is that the spin density at N^c is very small, 0.002 in ES1, ES2, and ES3. This magnitude is even smaller than previously calculated small values of 0.02[12,29] and

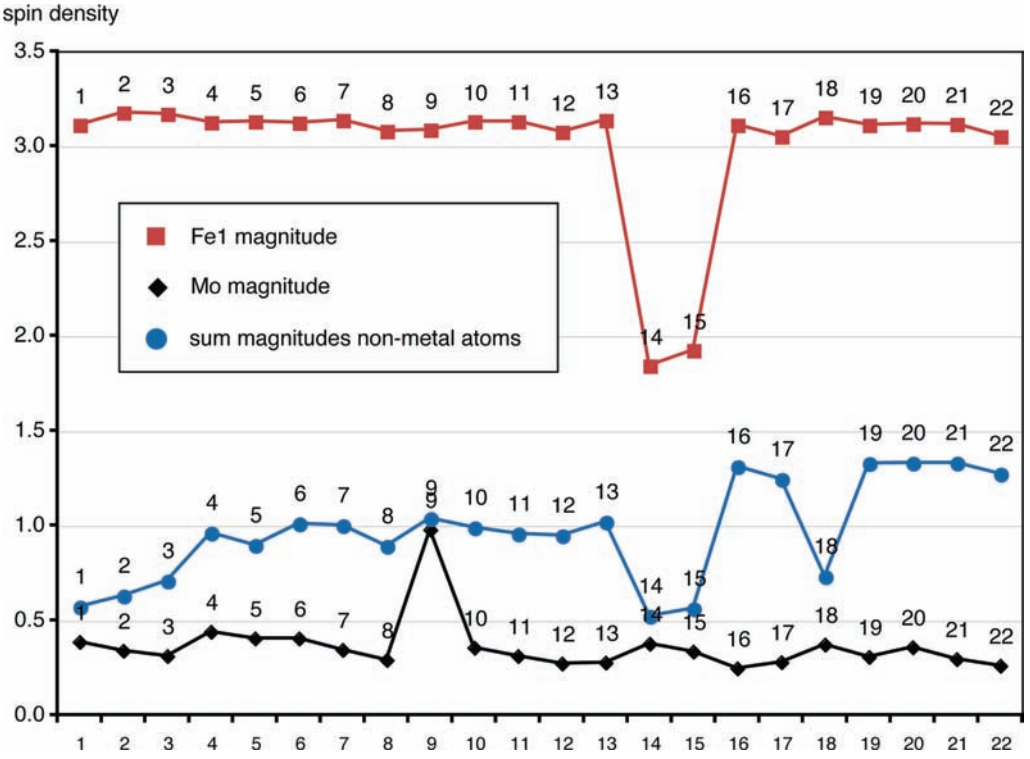

Figure 4. Absolute magnitudes of selected spin densities for the 22 more stable electronic states of FeMo-co (molecular spin $S = 3/2$), numbered according to spin-set as in Figure 3. Red is the magnitude of spin density on Fe1, black is the magnitude of spin density on Mo, and blue is the sum of the magnitudes of the spin densities on non-metal atoms. The connecting lines provide visual aid and have no physical meaning.

Table 1. Calculated Spin Densities for ES*n* ($n = 1-9$) of FeMo-co with $S = 3/2$

	ES1	ES2	ES3	ES4	ES5	ES6	ES7	ES8	ES9
Fe1	3.11	3.18	3.17	−3.13	−3.13	−3.12	−3.14	−3.08	3.09
Fe2	−2.89	−2.91	2.98	2.86	2.87	2.87	3.16	3.13	−2.80
Fe3	2.97	−2.93	−2.91	2.85	2.88	2.89	2.95	−2.94	−2.80
Fe4	−2.87	3.00	−2.88	2.84	2.79	2.85	−2.97	2.90	−2.76
Fe5	2.73	−2.76	2.70	−2.76	2.62	−2.79	2.76	−2.78	2.97
Fe6	2.70	2.68	−2.75	−2.74	−2.69	2.68	2.98	2.96	2.81
Fe7	−2.75	2.75	2.73	2.63	−2.77	−2.83	−2.77	2.79	2.94
Mo	−0.39	−0.34	−0.31	0.44	0.40	0.41	−0.34	−0.29	−0.98

0.03e,[47] and is consistent with the inability to detect any ENDOR signals attributable to N^c.[29] The S atoms of the cluster have spin densities ranging 0.01 to 0.13 in ES1, ES2, and ES3 ($S = 3/2$), while the S atom of the coordinated cysteine (Figure 1) has spin density magnitude in the range 0.14 to 0.16e for the 13 most stable ES states. Further details are provided in the Supporting Information.

How does the geometry of FeMo-co vary with its electronic state? The main geometrical variations occur at the central six Fe atoms Fe2−Fe7, and are best assessed in terms of the strongly bonding N^c−Fe distances rather than weakly bonding Fe−Fe distances. Details for the first 17 electronic states (as defined in Figure 3) for molecular spins $S = 3/2$, 1/2, and 5/2 are provided in Figure 5. In the most stable electronic states, ES1, ES2, and ES3 ($S = 3/2$) the mean N^c−Fe distance is 2.05 Å with dispersions (ranges) 0.06−0.08 Å. In most of the other less stable states the dispersions are about 0.2 to 0.3 Å. Note that for the lower molecular spin $S = 1/2$ the mean distances are generally smaller than for the higher spin states. Experimental comparison is best made with the most accurate crystal structure PDB code 1M1N, in which there are four crystallographically independent FeMo-co clusters.[3] The mean values for these are all 2.00 Å, and the dispersions in the independent clusters are 0.15, 0.12, 0.19, and 0.11 Å. There is a minor pattern of distance differences in these four experimental structures: Fe6−N^c is consistently longer (mean 2.07, std 0.02 Å) and Fe3−N^c (1.95, 0.03) and Fe4−N^c (1.96, 0.03) are consistently shorter, no doubt for reasons of protein influence, and accordingly this is not reflected in the calculated structures. The discrepancy of 0.05 Å between mean values calculated for stable states of FeMo-co and the mean experimental value indicates the magnitude of inaccuracy in the DMol procedure.

For FeMo-co and its derivatives, including ligated forms observed experimentally and those postulated in mechanistic sequences, there is the question of finding the most stable electronic state efficiently, without having to test the large number of possibilities. At this point I describe how the more stable electronic states of FeMo-co can be reached directly. The question is the minimal degree of pre-scf spin specification needed for the

(47) Hinnemann, B.; Norskov, J. K. *Top. Catal.* **2006**, *37*(1), 55–70.

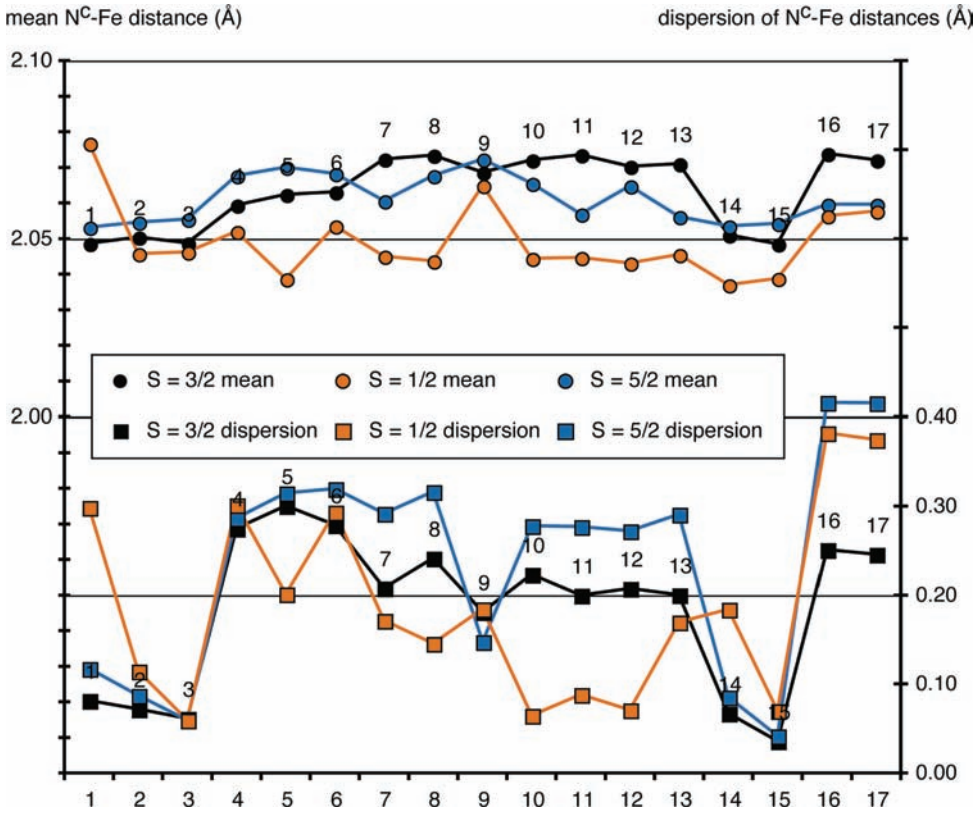

Figure 5. Statistics for the six N^c−Fe distances (Å) in the electronic states 1−17 for $S = 3/2$ (black), $S = 1/2$ (orange) and $S = 5/2$ (green). Circles are the mean N^c−Fe distance (left scale) and squares are the dispersion of the six distances, longest - shortest (right scale). The connecting lines are visual guides.

calculation to be able to reach the best electronic state. The above-described principles suggest that the pre-scf specifications should embody opposite signs for prism edges, or mixed signs in cubanoid fragments, and magnitudes about 3e for Fe. The following representative results for FeMo-co (all for $S = 3/2$ molecular spin) illustrate outcomes from minimal pre-scf specification: (a) various specifications of three Fe spins, for Fe1/Fe4/Fe5, or Fe2/Fe3/Fe4, or Fe5/Fe6/Fe7, yield one of the three top ranked states ES1, ES2, or ES3; (b) specification of four Fe spins on two prism edges, Fe3−Fe7/Fe4−Fe5, or Fe2−Fe6/Fe3−Fe7, yield one of the three top ranked states ES1, ES2, or ES3. In at least one case pre-scf specification with spin magnitudes of 1e rather than 3e resulted in the correct electronic state with spin magnitudes about 3e. The conclusion here is that the DMol scf calculation is fairly robust in locating the most favorable electronic states for a defined overall molecular spin, and that extensive testing is not need to locate the ground electronic state. Further results for the location of ground electronic states for derivatives of FeMo-co are presented below.

Intermediate I. This structure is a key intermediate in the proposed mechanism, being the first binding of N_2 after FeMo-co has been hydrogenated three times.[33] Intermediate **I** was labeled **3HN$_2$-a** in the published mechanism. Hydrogen atoms are bound at Fe2, S2B, and Fe6, and N_2 is bound in η^2 mode at the *endo* coordination position of Fe6, and so this is a good example to investigate the effects of these bound atoms on the spin densities of metal and sulfur atoms, and, conversely, the extent to which spin is delocalized onto bound N_2 and H. With net charge −3 intermediate **I** has an even number of electrons, and the likely molecular spin states are $S = 0$, 1, and 2.

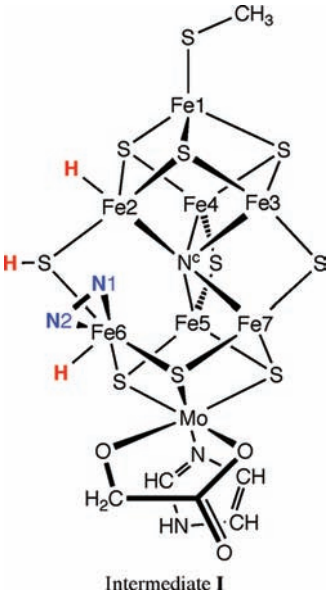

Intermediate **I**

The relative energies of the 32 more stable electronic states of intermediate **I** with $S = 0$, $S = 1$, or $S = 2$ are plotted in Figure 6. There are four $S = 0$ states and two $S = 1$ states within 1.5 kcal mol^{-1}, and the first $S = 2$ state occurs at +2 kcal mol^{-1}. All of these states have a geometry in which Fe6, coordinated by both H and N_2,

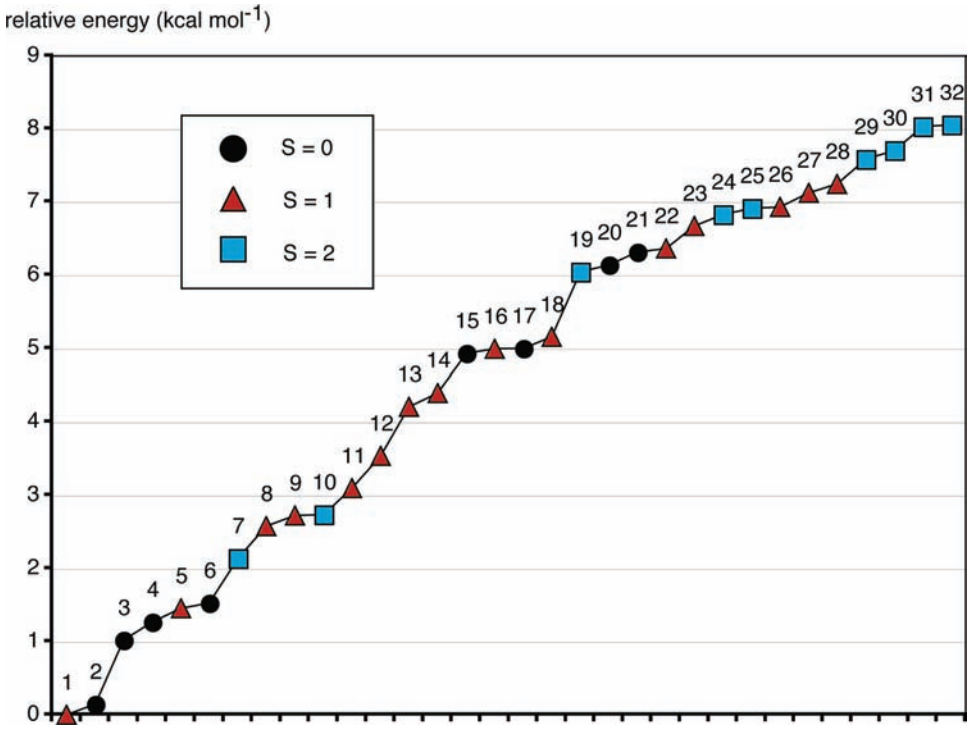

Figure 6. Relative energies (kcal mol^{-1}) of electronic states of intermediate **I**. Black circles are $S = 0$, red triangles $S = 1$, blue squares $S = 2$.

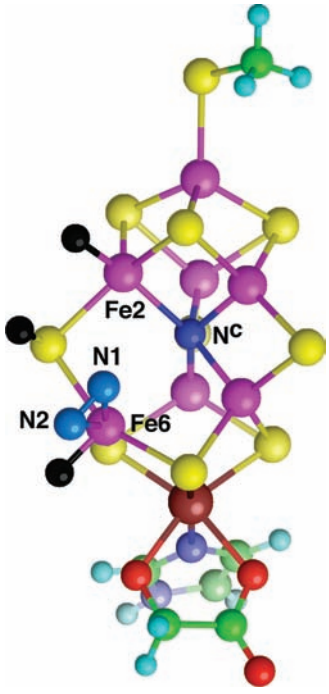

Figure 7. Structure of intermediate **I**, ES1. H atoms added during the mechanism are black.

is separated by about 3 Å from N^c. The coordination geometry at Fe6 is effectively square-pyramidal {(η^2-N_2)S_3H}. The structure of the most stable electronic state is pictured in Figure 7.

Calculated spin densities for the more stable electronic states are reported in Table 2. A remarkable result is that there is negligible spin density at Fe6 in all 32 electronic states: the largest magnitude for the spin density at Fe6 is 0.11e in ES4, and in most other states it is less than 0.05e. Fe6 is doubly ligated, distant from N^c, and has different coordination geometry (Figure 7),

Table 2. Calculated Spin Densities for ES1−ES6 of Intermediate **I**

	ES1	ES2	ES3	ES4	ES5	ES6
relative energy kcal mol^{-1}	0.00	0.14	1.02	1.27	1.46	1.53
molecular spin S	1	0	0	0	1	0
Fe1	3.04	3.04	3.08	3.08	3.05	3.08
Fe2	−2.08	−1.91	−2.23	−2.11	−1.81	−2.24
Fe3	−2.84	−2.98	2.75	−2.95	−2.63	2.74
Fe4	2.86	−2.95	−2.91	2.66	−2.59	−2.91
Fe5	−2.20	2.52	2.10	−2.83	2.91	2.13
Fe6	0.03	0.04	−0.01	−0.11	0.06	−0.03
Fe7	2.85	2.70	−2.85	2.32	3.00	−2.86
Mo	0.006	−0.545	0.030	0.048	−0.641	0.029
N imidazole	0.002	0.005	−0.002	0.002	0.006	−0.003
N imidazole	−0.001	0.000	0.001	0.000	0.000	0.001
N^c	0.020	−0.021	−0.029	−0.043	0.154	−0.031
O homocitrate	0.001	−0.002	0.000	0.003	−0.003	−0.001
O homocitrate	−0.023	−0.032	0.023	−0.017	−0.033	0.024
S cysteine	0.129	0.162	0.139	0.135	0.155	0.138
S1A	−0.016	−0.014	−0.053	−0.030	−0.020	−0.053
S2A	−0.041	−0.059	0.002	−0.050	−0.070	0.009
S3A	0.054	−0.087	−0.071	−0.040	0.059	−0.072
S4A	0.047	−0.111	0.073	0.048	−0.070	0.072
S1B	−0.014	0.067	0.013	−0.063	0.063	0.015
S2B	−0.003	−0.009	−0.029	−0.006	−0.010	−0.026
S3B	0.054	0.057	−0.050	0.009	0.063	−0.055
S4B	0.058	0.133	−0.069	−0.036	0.217	−0.069
S5A	−0.028	−0.100	−0.006	−0.127	0.051	−0.008
H−S2B	−0.001	−0.002	−0.002	−0.001	−0.003	−0.002
H−Fe2	0.089	0.098	0.100	0.089	0.109	0.101
H−Fe6	−0.001	−0.010	−0.003	0.005	−0.011	−0.001
N_2 N1	−0.002	−0.004	0.001	−0.001	−0.008	0.001
N_2 N2	−0.003	−0.005	0.004	0.003	−0.008	0.005

Table 3. Mean and Standard Deviations for Selected Distances in the 32 Electronic States of Intermediate **I**

distance	mean (Å)	standard deviation (Å)
N^c−Fe6	3.06	0.09
N^c−Fe2	2.16	0.06
N^c−Fe3	1.93	0.04
N^c−Fe4	2.00	0.08
N^c−Fe5	1.98	0.03
N^c−Fe7	2.05	0.05
N^c−N1	2.21	0.01
N^c−N2	2.26	0.02
Fe6−N1	2.21	0.01
Fe6−N2	2.26	0.02

and so a question arises as to which of these attributes diminish so strongly the spin density at Fe6. At Fe2, also exoligated by H, but closer (ca. 2.2 Å) to N^c, the spin density is about 2e in the more stable electronic states. Variable spin density, about 0.0 or about 0.5, occurs at Mo. The total magnitude of spin density on other atoms is in the range 0.6 to 1.3e, and, as in FeMo-co, most of this spin is on S atoms. At N^c the magnitude of the spin density is 0.02 in ES1 and ES2: the maximum spin density on N^c is 0.15 in ES5. The maximum spin density on either of the ligated N_2 atoms is 0.01e; on the H atom bound to Fe2 the maximum density is 0.11e, on H−Fe6 the maximum is 0.01e, and on H−S2B the spin density is calculated to be about 0.002e for all electronic states.

Pelmenschikov et al.[30] reported calculations on structures with allyl alcohol bound as η^2-C=C to Fe6, analogous to η^2-N≡N in **I**, without H atoms on Fe6, Fe2 and with H on S2B and S3A, and reduced overall by two-electrons. Spin populations were <0.1e on the alkene C atoms, and 0.02−0.04e at N^c. Two of the allyl alcohol bound structures have some relevance here because they retain S_3Fe6(C=C) coordination: one has shorter Fe6−N^c and smaller spin density (1.1) at Fe6, while the other has long Fe6−N^c and larger Fe6 spin density (3.0). These results appear to be inconsistent with the correlation of long N^c--Fe6(N_2) and very small Fe6 spin density found for intermediate **I**, but there are substantial geometrical differences (exo Fe6(C=C) vs endo Fe6(N≡N), and different SH conformations) as well as electronic population differences, which complicate comparisons.

Examination of the spin-sets for the more stable electronic states of **I** reinforces the above-stated stabilizing principles of antiparallel spins on the prism edges (only two edge pairs are relevant because the spin on Fe6 is almost zero) and 2 + 2− spins in the Fe-cubanoid moiety.

The geometry of **I** is largely invariant over the 32 electronic states, as demonstrated in Table 3. The Fe6−N distances are 2.20 and 2.26 Å in ES1, and 2.21(sd 0.01) and 2.26(sd 0.02) for all 32 electronic states.

Intermediate II. This is the intermediate after two H atoms have been transferred to the bound N_2 of intermediate **I**. In the published mechanism[33] this intermediate is labeled **3HN$_2$H$_2$-a**. Both H atoms were transferred via S3B, generating cis N_2H_2, in which the inner N1 atom forms an additional bridging bond with Fe2. The Fe2−N^c and Fe6−N^c distances are variable, and where they are sufficiently bonding, Fe2 and Fe6 have approximate octahedral coordination.

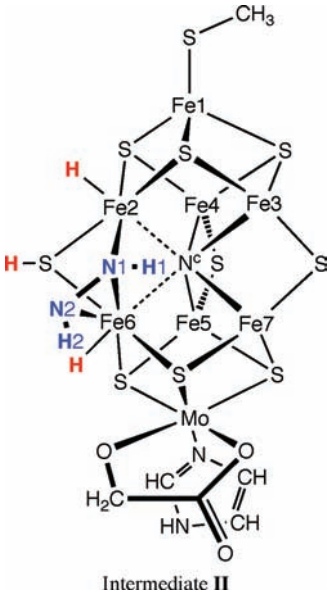

Intermediate **II**

For this intermediate 35 different electronic states encompassing molecular spin $S = 0$ and $S = 1$ have been calculated. The relative energies of the best 22 of these are graphed in Figure 8. The lowest energy state, ES1, is a spin triplet $S = 1$, separated by 2.4 kcal mol^{-1} from ES2 which is $S = 0$. Thirteen electronic states have energies within 6 kcal mol^{-1} of the ground state ES1. There is a clear correlation between stability and spin-sign combinations on central Fe atoms, but in this case only the spins of *unligated* Fe atoms Fe3, Fe4, Fe5, and Fe7 are important, in the following manner: the eleven best electronic states ES1 to ES11 have spin density magnitudes in the range 2.4 to 3.1e at Fe3, Fe4, Fe5, and Fe7, and all have +− combinations along the prismane edges Fe3−Fe7 and Fe4−Fe5. This reinforces the principles relating stability and appreciable Fe spin combinations introduced above for FeMo-co and intermediate **I**.

At the *ligated* Fe atoms Fe6 and Fe2 the magnitudes of the spin densities are consistently relatively small, not rising above 0.26e at Fe6, and ranging 0.5−1.0e at Fe2 for the more stable electronic states (Figure 9). At Mo the magnitude of the spin density varies between 0.9 and 1.5e. This general consistency of magnitude of spin density at metal atoms is broken at Fe1. In the two most stable electronic states ES1, ES2, spin density at Fe1 is about 3.2e, as in FeMo-co and intermediate **I**, but then diminishes to 0.1e in ES3 and fluctuates between very small and intermediate values in subsequent electronic states (see Figure 9). This suggests that the magnitude of the spin density at Fe1 is a minor determinant of stability, compared with the spin populations at the core metal atoms. At N^c the magnitude of the spin density is 0.048 in ES1, and is <0.10e in the first 11 electronic states.

Spin densities at the ligand atoms are universally small, being <0.04e at the diazene N atoms N1, N2, <0.01e at the

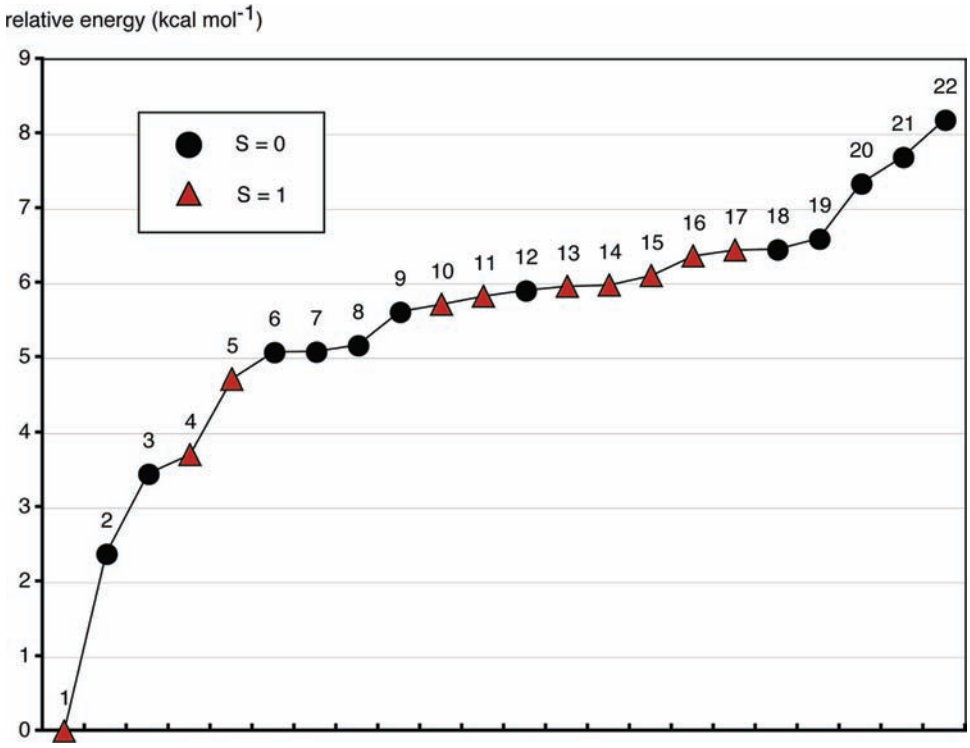

Figure 8. Relative energies (kcal mol^{-1}) of the 22 lower energy electronic states of intermediate **II**. Red triangles are $S = 1$ states, black are $S = 0$.

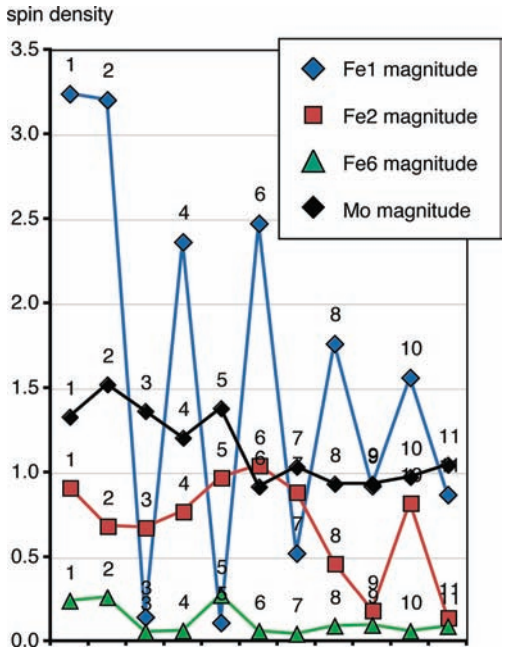

Figure 9. Magnitudes of the spin densities at Fe1, Fe2, Fe6, and Mo of ES1−ES11 of intermediate **II**. Electronic states are numbered as in Figure 8. The connecting lines are visual guides.

diazene H atoms, < 0.03e at H bound to Fe6, < 0.07e at H bound to Fe2, and <0.01e at H bound to S2B. Selected values are reported in Table 4, with full details in the Supporting Information.

I now describe significant geometrical properties of the electronic states of **II**. The structure of the most stable state (ES1 $S = 1$) is shown in Figure 10. In this and the structures of the other electronic states of **II** the coordination of *cis*-N_2H_2 to both Fe2 and Fe6 is unremarkable, with normal Fe−N, N−N, and N−H distances. The N^c−Fe6 and N^c−Fe2 distances are variable through the electronic states, as shown in Figure 11. In ES1 both distances are 2.45 Å, and in the higher energy states up to ES22 the average of these two distances remains relatively close to 2.45 Å (range 2.39−2.60 Å). However, the individual distances can deviate substantially from the average, with N^c−Fe2 smaller and down to 2.18 Å, and N^c−Fe6 larger and up to 2.95 Å. This variation can be regarded as a vertical sliding of the Fe2−N_2H_2−Fe6 moiety relative to N^c. These data also illustrate the phenomenon of coordinative allosterism in FeMo-co,[22] in which there is communication between Fe atoms via their degree (i.e., length) of bonding with N^c, although in the case of **II** Fe2 and Fe6 are linked through N1 as well as N^c. There is no evident correlation of the N^c−Fe distances with molecular spin or with atomic spin density on Fe2, Fe6.

Intermediate III. Intermediate **III** is FeMo-co with H atoms bound in the *exo* coordination positions of Fe2 and Fe6, H bound to S2B, N_2 bound end-on (η^1) at the *endo* coordination position of Fe6, and an H atom bound to S3B. This intermediate is not postulated to be involved in the mechanism for the hydrogenation of N_2 to NH_3,[33] but it is postulated[48] as an intermediate in the reaction $D_2 + 2H^+ + 2e^- \rightarrow 2HD$ which is effected by nitrogenase in the presence of N_2. In the present context it is representative of many postulated intermediates containing hydrogenated S3B, which arise when a proton is transferred to electronated FeMo-co. It is proposed[20−22,33] that the proton is transferred from

(48) Dance, I., *in preparation for publication* **2010**.

Table 4. Spin Densities on Selected Atoms of Intermediate **II**

	ES1	ES2	ES3	ES4	ES5	ES6	ES7	ES8
molecular spin *S*	1	0	0	1	1	0	0	0
H−Fe6	0.007	0.003	−0.005	−0.006	−0.008	−0.003	0.000	0.012
H2	0.000	0.000	0.000	0.000	0.000	−0.001	−0.001	−0.001
H−S2B	0.001	0.001	−0.001	−0.001	−0.002	0.001	0.000	0.000
H−Fe2	0.062	0.028	−0.027	−0.026	−0.060	0.071	−0.044	0.007
H1	0.003	0.003	−0.001	0.001	−0.001	0.001	−0.005	0.003
N-imidazole bound	0.012	0.014	0.012	0.011	−0.012	0.008	0.006	0.010
N-imidazole	−0.002	−0.002	−0.002	−0.001	0.002	−0.001	−0.002	−0.002
N^c	0.048	−0.101	0.088	0.057	−0.055	0.007	0.053	−0.020
N1	0.025	0.020	−0.007	−0.016	−0.020	0.010	−0.009	−0.006
N2	0.029	0.036	−0.022	−0.027	−0.035	0.010	−0.015	0.007
O homocitrate	−0.01	−0.01	−0.01	−0.01	0.01	−0.01	−0.01	0.00
O homocitrate	−0.02	−0.02	−0.02	−0.02	0.02	−0.03	0.03	−0.01
S cysteine	0.17	0.18	0.01	0.10	0.00	0.11	−0.02	0.09
S1A	0.11	0.10	−0.14	−0.13	0.12	−0.12	0.04	−0.06
S2A	0.06	0.05	−0.14	−0.10	0.12	−0.10	0.15	−0.11
S3A	0.01	−0.14	−0.01	0.01	0.00	−0.01	0.02	0.01
S4A	−0.04	−0.10	−0.13	−0.17	0.14	−0.21	0.09	0.01
S1B	0.11	0.11	0.11	0.11	−0.11	0.08	0.10	−0.07
S2B	0.02	0.00	−0.01	0.00	0.01	0.02	−0.02	0.00
S3B	0.09	0.10	0.09	0.08	−0.09	0.07	−0.11	0.07
S4B	0.22	0.14	0.23	0.22	−0.22	0.19	0.02	0.03
S5A	0.01	−0.15	−0.01	−0.01	−0.01	−0.04	0.03	−0.01

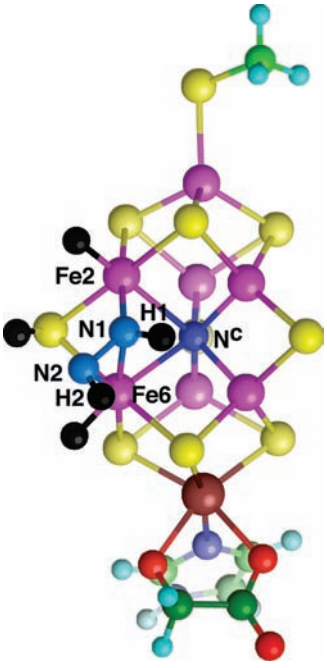

Figure 10. Structure of the most stable state ES1 for intermediate **II**. H atoms added during the mechanism are black.

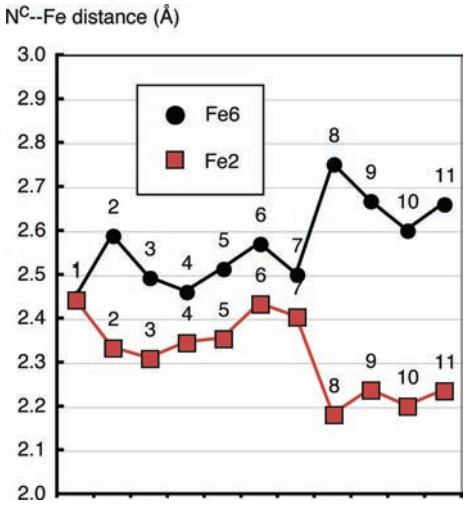

Figure 11. Variation of the N^c−Fe2 and N^c−Fe6 distances(Å) in the 11 more stable electronic states of intermediate **II**. Connecting lines are visual guides.

a water molecule at the terminus of the proton transfer chain (HOH679 in PDB structure 1M1N) in the direction that leads first to structure **A**, which is followed by conformational changes at S3B through structure **B**, and on to structure **C**, from which the H atom is able to transfer to other atoms of FeMo-co, or to bound intermediates. Conformations **A**, **B**, and **C** correspond to the conformations denoted **S3BH-5**, **S3BH-4**, and **S3BH-3**, respectively, in the previous fuller discussion of the conformational possibilities at S3B.[20]

This structural variation at S3B follows established paradigms of coordination chemistry. Atom S3B bridges three metal atoms in FeMo-co. When S3B bears a hydrogen atom and becomes nominally four coordinate, one of these S3B-metal bonds can be weakened such that S3B−H approaches a doubly bridging SH structure. By analogy with metal thiolates,[49] triply bridging-, doubly bridging-, and terminal-SH ligand functions are all feasible, but μ_3-SH functions are relatively rare in the literature, while μ-SH is well established.[50] Thus the literature supports the postulated weakening of one of the S3B−Fe6, or S3B−Fe7, or S3B−Mo bonds when FeMo-co is hydrogenated at S3B. This elongation of an HS3B-metal interaction allows a variety of detail in the bonding around S3B−H, as has been found in calculated structures of the intermediates investigated and reported previously.[20,33] Figure 12 shows detail of

(49) Dance, I. G. *Polyhedron* **1986**, *5*, 1037–1104.
(50) Kuwata, S.; Hidai, M. *Coord. Chem. Rev.* **2001**, *213*(1), 211–305.

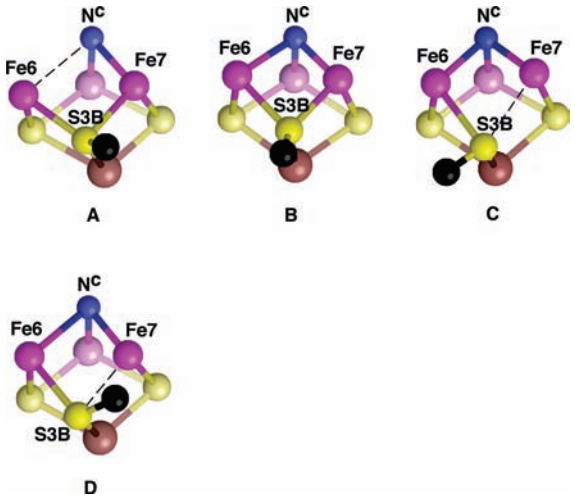

Figure 12. Details of the conformations of S3B−H (H black) as they occur in intermediate **III**. Broken lines signify long interatomic distances.

the four conformations, **A**, **B**, **C**, and **D** reported here for intermediate **III**.

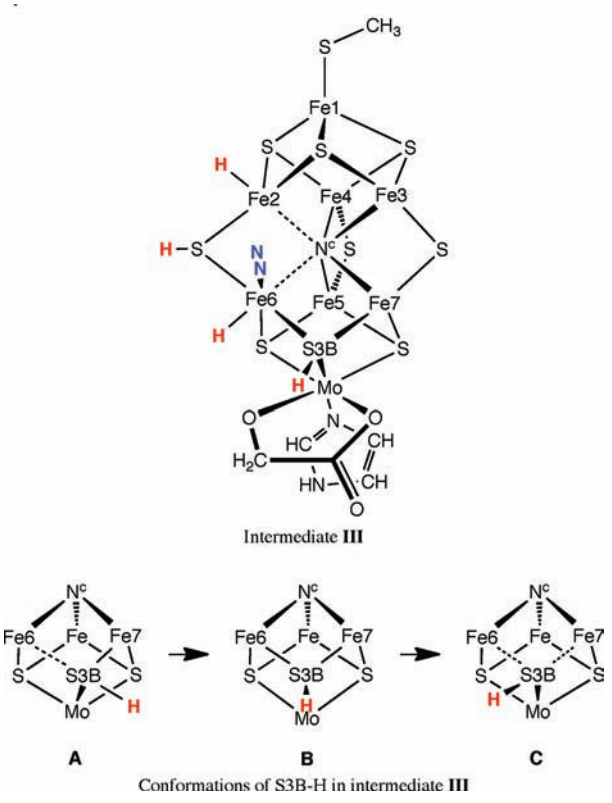

Here the question investigated is the relationship between electronic structure and geometrical structure of **III**. Because the variation of energy with conformation at S3B−H is relatively small, different electronic states of **III** may influence this conformation, as well as influencing N^c−Fe bonding distances as seen above.

The calculational procedure was to start with a minimized structure in conformation **B**, and optimize it with each of the favorable spin sets already identified for FeMo-co and other intermediates, for overall molecular spin states $S = 1/2$ or $S = 3/2$. Thirty unique results were

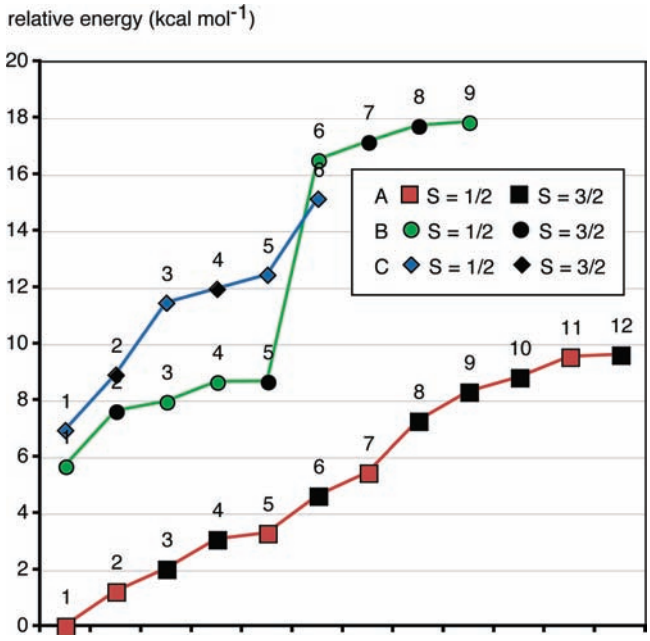

Figure 13. Relative energies (kcal mol^{-1}) of the electronic states of intermediate **III** in conformations **A** (red), **B** (green), and **C** (blue). Open symbols are $S = 1/2$, closed symbols are $S = 3/2$ molecular spin states, connecting lines are visual guides.

obtained, 9 in which conformation **B** was retained, 14 in which the structure changed to conformation **A**, 6 which changed to conformation **C**, and one anomalous conversion to conformation **D**. The relative energies of the lowest energy 26 of these states for conformations **A**, **B**, **C** are plotted in Figure 13. The best seven electronic states of conformation **A** are lower in energy than any states of conformation **B**, and the five more favorable conformation **B** electronic states are lower energy than all but one of the conformation **C** states. The numbering of electronic states for each conformation is according to energy ranking, and (as usual in this paper) does not signify equivalent spin-sets, and therefore the data in Figure 13 cannot be read directly in terms of energy trajectories for transformations between the conformations on the same potential energy surface. The calculation of trajectory from **A** to **B** to **C** as a key preparatory component of the hydrogenation mechanism[33] is different, and involves specification of one electronic state (spin-set) to locate the transition state between **A** and **B** using the method previously described,[32] specifying the same electronic state to locate the transition state between **B** and **C**, and then following (by small-step energy minimization) the paths from these transition states to the connected energy minima for intermediates **A**, **B**, and **C**.

Within each of the conformations the geometries of the different electronic states vary little. Key distances and angles are tabulated in Table 5, as averages and standard deviations of the collections of electronic states for each conformation. Each conformation has distinctive properties: for **A**, H−S3B−Fe7 is smaller and Fe6−N^c is long; for **B**, H−S3B−Fe7 is larger and Fe2−N^c is long; for **C**, S3B−Fe7 and Fe2−N^c are long. Note that the standard deviations of the distances and angles around S3B are all quite small, about 0.02 Å, 3°. The standard deviations for the Fe−N^c distances are slightly larger, 0.03−0.14 Å.

For conformation **A** the less stable electronic states ES9, ES10, ES11, and ES12 are different from the remainder, in that Fe2−N^c is longer, 2.56−2.82 Å, compared with 2.18(0.06)Å. ES1 of conformation **C** also differs from the other five electronic states, with Fe6−N^c = 2.55 Å rather than 2.24 (0.03)Å. The one instance of the fourth conformation **D** has relative energy +7 kcal mol^{-1}: its distinctive geometry (Table 5) is the small angle H−S3B−Fe7.

Spin densities for the five most stable electronic states of each conformer are contained in Table 6. Note that the magnitude of the spin density at Fe6 is about 0.03e in all of the more stable electronic states for all three conformations, and does not exceed 0.14e in the less stable states. At Fe2 the magnitude of the spin density is generally in the range 1.6−2.1e (**A**:ES5 is exceptional). There is no correlation between the spin density at Fe6 or Fe2 and the corresponding Fe−N^c distances: rather, it is the ligation of Fe6 by N_2 and H which correlates with the negligible spin density at Fe6. The magnitude of the spin density at Fe1 is about 3e. At the other non-ligated Fe atoms Fe3, Fe4, Fe5, Fe7, the magnitudes of the spin densities are generally in the range 2.5−3e, although **A**:ES2 is anomalous with +0.03e at Fe3. The results for intermediate **III** are consistent with the precepts already noted for spin-sign combinations, namely, that favorable energies are associated with antiparallel signs for the prismane edges Fe3−Fe3 and Fe4−Fe5, and 2 + 2− combinations in the Fe1-cubanoid moiety.

Table 5. Average Distances (Å) and Angles (deg), with Standard Deviations in Parentheses, for the Electronic States of the Conformations of **III**

	A	B	C	D
S3B−Fe6	2.33 (0.01)	2.37 (0.01)	2.50 (0.04)	2.43
S3B−Fe7	2.41 (0.03)	2.38 (0.01)	2.92 (0.07)	2.58
S3B−Mo	2.49 (0.02)	2.48 (0.01)	2.53 (0.01)	2.56
H−S3B−Fe6	127 (2)	119 (3)	93 (3)	111
H−S3B−Fe7	103 (5)	143 (4)	157 (2)	58
H−S3B−Mo	128 (2)	124 (2)	94 (1)	109
Fe6−N^c	3.10 (0.11)[a]	2.44 (0.06)	2.24 (0.03)[b]	2.51
Fe2−N^c	2.18 (0.06)[a]	2.90 (0.06)	2.84 (0.14)[b]	2.11

[a] Excluding ES9, ES10, ES11, ES12: see text. [b] Excluding ES1: see text.

At Mo the spin density is variable: note the values 1.58, 0.14, −1.59, 0.00, −1.61 for states ES1 to ES5 of conformer **A**. One significant observation is that the spin density at Mo is the only variable in some pairs of $S = 1/2$ and $S = 3/2$ states. Thus, for conformer **A**, ES10 ($S = 1/2$) and ES11 ($S = 3/2$) have very similar spin densities on all atoms except Mo, where they are −0.06 and +1.55e respectively. For conformer **B**, ES4 ($S = 1/2$) and ES5 ($S = 3/2$) are virtually identical in relative energy, geometry, and spin densities on all atoms, except Mo spin densities of −1.34 and +0.88e, respectively. The pairs ES6 and ES7 of conformer **B**, and ES4, ES5 of conformer **C**, are similarly related. In these cases spin flip at Mo does not influence the energy of an electronic state.

In all electronic states of intermediate **III** the spin densities at S3B are less than 0.09e, and at H bonded to S3B are ≤0.01e. At H on Fe2 the spin density is about 0.1e, while at the H atom bound to Fe6 the spin density is an order of magnitude smaller, ≤ 0.01e. The spin densities on the proximal and distal N atoms of η^1-bound N_2 are universally < 0.01e.

The question of ability to find the more stable electronic states readily without testing all conceivable possibilities was also investigated for intermediate **III**, through trial calculations with minimal pre-scf spin sets. Specifications of spin-sets for only Fe1, Fe2, Fe3, Fe4 yielded A:ES2, B:ES2, B:ES3, and A:ES4; specifications of spin-sets for only Fe3, Fe4, Fe5, Fe7 yielded A:ES1, B:ES2; specifications of spin-sets for only Fe1, Fe3, Fe4, Fe5 yielded B:ES3, A:ES6.

Table 6. Atomic Spin Densities for the More Stable Electronic States of Conformers **A**, **B**, and **C** of Intermediate **III**

	A:ES1	A:ES2	A:ES3	A:ES4	A:ES5	B:ES1	B:ES2	B:ES3	B:ES4	B:ES5	C:ES1	C:ES2	C:ES3	C:ES4	C:ES5
molecular spin S	1/2	1/2	3/2	3/2	1/2	1/2	3/2	1/2	1/2	3/2	1/2	3/2	1/2	3/2	1/2
Fe1	−3.05	3.03	3.10	2.96	3.07	2.99	3.05	3.05	3.06	3.05	−3.00	−3.04	3.02	2.96	2.95
Fe2	1.91	−1.92	−1.99	−1.66	0.11	−1.55	−1.88	−1.88	−1.94	−1.91	2.01	1.82	−1.77	−1.86	−1.83
Fe3	3.02	−2.97	0.03	−2.80	−3.04	−2.73	2.99	2.98	−2.71	−2.75	2.82	2.78	−2.98	2.81	2.80
Fe4	2.95	−2.95	−2.68	−1.90	−3.00	−2.67	−2.75	−2.76	2.90	2.90	−2.86	2.79	2.49	−2.76	−2.76
Fe5	−2.66	2.70	2.82	2.93	2.70	2.98	2.64	2.77	−2.38	−2.56	2.36	−2.46	1.64	−2.27	−1.80
Fe6	0.02	0.03	−0.02	0.04	−0.02	−0.02	0.03	−0.11	−0.01	0.13	−0.02	−0.04	−0.01	0.10	0.01
Fe7	−2.78	2.83	2.85	2.96	2.78	3.06	−2.81	−2.70	2.93	2.85	1.57	2.58	−2.84	2.54	2.69
H−S3B	0.01	0.01	−0.01	0.01	−0.01	0.01	−0.01	−0.01	0.01	0.01	−0.01	−0.01	0.00	0.00	0.00
H−Fe2	−0.10	0.11	0.09	0.10	−0.01	0.10	0.11	0.11	0.10	0.10	−0.10	−0.12	0.10	0.11	0.11
H−Fe6	0.00	−0.01	0.00	−0.01	0.00	0.01	−0.01	0.01	0.00	−0.01	0.00	0.01	−0.01	−0.01	0.00
Mo	1.58	0.14	−1.59	0.00	−1.61	−1.71	1.31	−0.81	−1.34	0.88	−1.71	−1.46	1.30	1.32	−1.38
N imid coord	−0.02	0.00	0.02	0.00	0.02	0.02	−0.02	0.01	0.02	−0.01	0.02	0.02	−0.01	−0.01	0.01
N imid	0.00	0.00	0.00	0.00	0.00	0.00	0.00	0.00	0.00	0.00	0.00	0.00	0.00	0.00	0.00
N^c	0.03	−0.03	0.04	0.07	−0.04	0.11	−0.01	0.00	0.05	0.03	−0.09	−0.03	−0.01	0.02	0.00
N distal	0.00	0.00	0.00	0.00	0.00	0.00	0.00	0.01	0.00	0.00	0.00	0.01	0.00	−0.01	0.00
N proximal	0.00	0.00	0.00	0.00	0.00	0.00	0.00	0.00	0.00	0.00	0.00	0.00	0.00	0.00	0.00
O homocit	0.01	0.01	−0.01	0.00	−0.01	−0.01	0.01	−0.01	−0.01	0.01	−0.01	−0.01	0.01	0.01	−0.01
O homocit	0.04	−0.04	−0.04	−0.03	−0.04	−0.06	0.05	0.06	−0.06	−0.06	−0.06	−0.06	0.04	0.02	−0.04
S cysteine	−0.16	0.16	0.16	0.15	0.15	0.16	0.15	0.15	0.14	0.14	−0.14	−0.16	0.14	0.14	0.14
S1A	0.02	−0.01	−0.02	−0.01	0.03	−0.03	−0.03	−0.03	0.02	0.03	0.04	0.04	−0.01	−0.01	0.00
S2A	0.07	−0.07	0.01	−0.05	0.00	−0.07	0.09	0.09	0.00	−0.01	0.00	0.03	0.02	0.03	0.02
S3A	0.14	−0.12	−0.12	−0.02	−0.13	0.05	0.08	0.09	−0.03	−0.03	−0.06	0.01	0.22	−0.35	−0.27
S4A	0.12	−0.12	0.03	0.00	−0.12	−0.10	0.10	0.10	0.08	0.07	−0.05	0.09	0.04	0.08	0.08
S1B	−0.07	0.10	0.07	0.10	0.07	0.08	0.07	0.04	−0.06	−0.02	0.08	−0.04	−0.01	−0.04	−0.02
S2B	0.01	−0.02	−0.01	−0.01	0.01	−0.01	−0.01	−0.02	0.00	0.00	0.00	0.02	−0.01	−0.01	−0.01
S3B	−0.08	0.05	0.06	0.05	0.09	0.08	−0.08	−0.07	0.08	0.07	0.01	0.01	−0.01	0.02	0.02
S4B	−0.11	0.10	0.13	0.13	0.12	0.20	−0.03	0.04	0.04	−0.03	0.04	0.01	−0.03	−0.08	0.05
S5A	0.07	−0.07	0.13	−0.02	−0.07	0.14	−0.12	−0.08	0.15	0.09	0.22	0.27	−0.39	0.21	0.30

Discussion

Exploration and Control of the Electronic States of FeMo-co and Derivatives. Operationally, the DMol methodology described here allows straightforward and simple calculation of the electronic states of FeMo-co and its derivatives. All that is required is specification of the signs and approximate magnitudes of pre-scf spin densities on metal atoms of FeMo-co, specification of overall molecular spin S, and energy optimization. This is valuable in two applications. Where a particular electronic state is to be maintained, as for instance in calculations of reaction trajectories and transition states, specification of a fuller spin-set involving a majority of the metal atoms in FeMo-co ensures that the electronic state is invariant and that a single potential energy surface is being investigated. Alternatively, where the electronic states occurring for a new derivative of FeMo-co are to be explored, and the lowest energy state is sought, testing a relatively small number of spin-sets involving spin-sign combinations for fewer metal atoms allows the low energy states to be found. This exploration for the lower energy electronic states is aided by knowledge of general principles reported in this paper: (i) antiparallel spins for Fe3−Fe7 and Fe4−Fe5 on the axial edges of the central Fe_6 prism are stabilizing; (ii) spin-densities on ligated Fe atoms (Fe6 and/or Fe2) are low magnitude, and so specification of them is not important; (iii) low net spin in the cubanoid moieties, particularly the Fe1 cube, is favorable, so 2 plus 2 opposing spins or 1 plus 3 opposing spins are stabilizing; (iv) specification of Mo spin density can be excluded from explorations because its spin density, sign and magnitude, appears to be more variable than spin density for Fe, with lesser influence on energy; (v) specification of pre-scf spin densities on non-metal atoms is unimportant.

The results presented are for FeMo-co and derivatives devoid of protein surrounds. Lovell et al.[27] have calculated that protein surrounds can modify relative energies of electronic states by up to 6 kcal mol^{-1}. For intermediate **I** eighteen electronic states encompassing three different molecular spin states are within 6 kcal mol^{-1} of the lowest energy state (and thirteen for intermediate **II**), and therefore caution must be exercised in drawing conclusions about the ground state. Some low-lying electronic states could be thermally accessible.

Previous tests have shown, at least for the tested systems, that the energy profile for a fundamental reaction such as association/dissociation of reactants (N_2, H_2) or H atom transfer from FeMo-co to bound N_2 or N_2H_x is not very dependent on the electronic/spin state.[33] However, as demonstrated in this paper for **III**, the steps in which H transfers to S3B and then moves around it can be affected by the electronic state of the reactants. The control of electronic states and potential energy surfaces via pre-scf densities is an essential component of simulations of reaction steps and intermediates in postulated mechanisms for the reactions of FeMo-co.

Distribution of Spin Density. Key significance attaches to the distribution of spin density over the atoms of FeMo-co and its ligated forms occurring as intermediates in its catalytic cycles. When Fe is coordinated by N_2 (η^2 or η^1) its spin density drops to a very low value (ca. 0.05e), compared with spin densities of order 2 or 3e at other Fe atoms. Spectroscopically, this obscures if not hides the Fe atom of most relevance. In intermediate **II** where there is bridging of N_2H_2 between two Fe atoms the spin densities on these Fe atoms are less diminished, but are still smaller than the spin densities on the unligated Fe atoms. A question that arises is "what is the principal cause of reduced spin density at any Fe?" Although only a limited number of different species are reported here, it is notable that in **II** there is no correlation of the N^c−Fe distances with atomic spin density on Fe2, Fe6. It is postulated that the ligation of Fe is more strongly correlated with spin density. At Fe2 with only exo-H in **I**, spin density is about 2e, while in **II** where there is additional ligation at the endo position of Fe2, the spin at Fe2 drops to less than 1e. The low spin density at Fe6 in **I**, **II**, and **III** appears to be primarily a consequence of its ligation.

Mo functions as a spin sink in FeMo-co, with quite variable spin, but, since Mo is most probably not directly involved in coordinated intermediates, this may be of little consequence.

More important is the distribution of spin density onto the N_2 and N_2H_x fragments bound to FeMo-co in intermediates. In **I** this spin density is < 0.01e on N; in **II** it is < 0.04e on N or H; in **III** it is < 0.01e on N. This has markedly negative ramifications for spectroscopic investigations that depend on electron spin density. H atoms bound to Fe have spin densities up to 0.12e (but generally much smaller), and H atoms bound to S atoms of FeMo-co have spin densities up to 0.09e (but often < 0.01e), properties which again diminish their prospects for detection. There is a tough irony in the general distribution of spin density over FeMo-co and its derivatives: the less interesting atoms get the spin, and the most interesting atoms do not.

Connections with Other Theoretical and Experimental Results. As already stated, the most stable electronic state for resting FeMo-co is calculated to be the same (ES1 = BS7) by the various theoretical methodologies. All calculations of the magnitudes of the spin densities on Fe atoms of FeMo-co yield similar results.[29,39] The spin density at N^c is calculated here to be even lower (0.002e) in ES1 than in other calculations (0.02,[12,29] 0.03e[47]). It is understandable that there has not yet been definitive experimental identification of the atom at the center of FeMo-co.[29]

At the Mo atom of FeMo-co, in resting[51,52] and reduced states,[52] the isotropic hyperfine coupling constant a_{iso} is measured to be of order 4−6 MHz. This is much lower than values (ca. 100 MHz) for related mononuclear Mo complexes,[53] and very much lower than free Mo atoms,[54] implying small spin densities (< 0.05e) on Mo in FeMo-co. The calculated spin densities on Mo for the more stable electronic states of resting FeMo-co are larger, 0.3−0.4e, and more detailed investigation of this aspect of electronic structure is needed: possibly relevant

(51) Venters, R. A.; Nelson, M. J.; McLean, P. A.; True, A.; Levy, M. A.; Hoffman, B. M.; Orme-Johnson, W. H. *J. Am. Chem. Soc.* **1986**, *108*, 3487–3498.

(52) Lukoyanov, D.; Yang, Z.-Y.; Dean, D. R.; Seefeldt, L. C.; Hoffman, B. M. *J. Am. Chem. Soc.* **2010**, *132*(8), 2526.

(53) George, G. N.; Bray, R. C. *Biochemistry* **1988**, *27*(10), 3603–3609. Wilson, G. L.; Greenwood, R. J.; Pilbrow, J. R.; Spence, J. T.; Wedd, A. G. *J. Am. Chem. Soc.* **1991**, *113*, 6803–6812. Drew, S. C.; Hanson, G. R. *Inorg. Chem.* **2009**, *48*, 2224–2232.

(54) Weil, J. A.; Bolton, J. R. *Electron Paramagnetic Resonance. Elementary Theory and Practical Applications*; Wiley-Interscience: New York, 2007.

in this context is the present result that calculated spin densities on Mo in derivatives of FeMo-co can be highly variable between close-lying electronic states.

In recent years there have been a number of EPR and ENDOR investigations of species trapped during turnover of wild-type and modified nitrogenases, and which are interpreted to be important intermediates. ^{15}N hyperfine interactions for trapped intermediates in experiments with N_2, CH_3NNH, and N_2H_4 range from 0.9 to 1.9 MHz.[6,16,18,55] The free atom hyperfine interaction for ^{15}N is 2540 MHz,[54] implying spin densities on the intermediate N atoms of order 0.004−0.007e, which is consistent with the calculated spin densities ranging from 0.001 to 0.036e on the N atoms in the electronic states of intermediates **I**, **II**, and **III**. Experimental isotropic ^1H hyperfine interactions for a trapped intermediate containing H atoms (described as $H^{\pm}$),[17] are 22, 24 MHz, which, relative to free ^1H atoms,[54] scale to spin density of 0.02e. Again this is generally consistent with the magnitudes of the calculated spin densities on H atoms bound to Fe or S in intermediates **I**, **II**, and **III**, which also contain other ligands. Experimental hyperfine interactions attributed to ^1H atoms on the ligands of trapped intermediates in experiments with $H_2C=CH-CH_2OH$, $CH_3N=NH$, and N_2H_4 range from 4 to 14 M Hz,[16,56] scaling to spin densities up to 0.01e: the calculated spin densities of comparable diazene H atoms in intermediate **II** are ≤0.003e, and so again there is broad agreement between calculated and experimental very low spin densities.

Conclusions

There are two main conclusions. (1) The computational methodology detailed here enables straightforward and efficient management of the electronic states of FeMo-co and its derivatives during simulations of its catalytic reactions. (2) There is a tough irony in the general distribution of spin density over FeMo-co and its derivatives: the less interesting atoms get the spin, and the most interesting atoms do not.

Acknowledgment. This research is funded by the Australian National Computational Infrastructure, and the University of New South Wales.

Supporting Information Available: Further details about the energy, spin density, and distance data for electronic states of FeMo-co. This material is available free of charge via the Internet at http://pubs.acs.org.

(55) Barney, B. M.; Laryukhin, M.; Igarashi, R. Y.; Lee, H.-I.; Dos Santos, P. C.; Yang, T.-C.; Hoffman, B. M.; Dean, D. R.; Seefeldt, L. C. *Biochemistry* **2005**, *44*, 8030–8037.

(56) Lee, H.-I.; Igarashi, R.; Laryukhin, M.; Doan, P. E.; Dos Santos, P. C.; Dean, D. R.; Seefeldt, L. C.; Hoffman, B. M. *J. Am. Chem. Soc.* **2004**, *126*, 9563–9569. Barney, B. M.; Lukoyanov, D.; Yang, T.-C.; Dean, D. R.; Hoffman, B. M.; Seefeldt, L. C. *Proc. Natl. Acad. Sci. U.S.A.* **2006**, *103*(46), 17113–17118.